Fabrication and characterization of Ag-SiO_2 composite hollow nanospheres

LI-MIN XU
Key Lab for Nanomaterials, Ministry of Education, Beijing University of Chemical Technology, Beijing 100029, People's Republic of China

JIE-XIN WANG
Research Center of the Ministry of Education for High Gravity Engineering and Technology, Beijing University of Chemical Technology, Beijing 100029, People's Republic of China

LI-XIONG WEN*
Key Lab for Nanomaterials, Ministry of Education, Beijing University of Chemical Technology, Beijing 100029, People's Republic of China

JIAN-FENG CHEN*
Key Lab for Nanomaterials, Ministry of Education and Research Center of the Ministry of Education for High Gravity Engineering and Technology, Beijing University of Chemical Technology, Beijing 100029, People's Republic of China
E-mail: chenjf@mail.buct.edu.cn

Published online: 12 January 2006

Ag-SiO_2 composite hollow nanospheres were synthesized by impregnation of hollow silica nanospheres (HSNSs), which were prepared by templating $CaCO_3$ nanoparticles, in $[Ag(NH_3)_2]NO_3$ aqueous solution followed by heat treatment. The straightforward process generates composite materials containing Ag nanoparticles, with the average size of 6–10 nm in diameter, uniformly dispersed and mainly distributed on the shells or between the spaces of the HSNSs. The Ag-supported HSNSs were characterized through TEM, EDS, and XPS. Furthermore, ASS, XRD and UV-Vis analyses demonstrated that higher loading efficiency could be achieved under the optimum loading conditions of a silver precursor solution of 0.08 M, pH = 9.0 and HSNSs with a BET surface area of 830.4 m^2/g.

1. Introduction

As a novel class of materials, hollow spheres have recently attracted great attentions due to their appealing structural design for many applications in catalysis, controlled release for drugs, dyes and perfumes, and protection of biologically active agents [1, 2]. To date, a variety of chemical and physicochemical methods [3–5] have been employed to produce hollow spheres comprised of various materials [6–11]. Sacrificial colloid particles, including mainly organic templates (polystyrene latex spheres, resin spheres, liquid droplets, vesicles, and microemulsion) [8, 9, 12–14] and inorganic templates (silica, silver and CS_2) [15–17], have been recognized as attractive alternative templates to generate hollow-sphere structures.

Nanoparticles of noble metals have potential applications in catalysis, optics, optoelectronics, and so on. However, unsupported nanoparticles are thermally unstable. Hence, the immobilization of these nanoparticles on the supports, such as polymer latex particles [18], alumina [19], zeolite [20], carbon cages [21], and porous silica (mesoporous silica, silica film and silica glass) [22–24], to form composite particles is of great interest. However, studies on noble metal particles immobilized on the surface of hollow nanoparticles have seldom been reported. When noble active components are supported on the porous shells of hollow structures, egg-shell heterogeneous catalysts can be easily achieved, which can be obtained on other porous solid materials just by controlling and changing loading conditions. The

*Author to whom all correspondence should be addressed.
0022-2461
DOI: 10.1007/s10853-005-2218-y

originally designed and fabricated architecture may exhibit some new opportunities for improving the performance of the catalysts. Compared with homogeneous catalysts, this structure feature will enhance the apparent activity, selectivity and anti-poisoning of catalysts greatly for some hydrogenation and oxidation reaction processes. This egg-shell distribution of catalyst will own the highest catalytic activity especially for fast reactions with strong diffusional restrictions and give higher selectivities for consecutive reactions.

Previously, we successfully obtained uniform nanosized $CaCO_3$ particles by a unique high gravity reactive precipitation (HGRP) method [25]. Here, we firstly reported the preparation of Ag-SiO_2 composite hollow nanospheres by adopting hollow silica nanospheres (HSNSs), which were fabricated via a $CaCO_3$ template route [26], as a support for immobilization of Ag nanoparticles by thermal treatment of $[Ag(NH_3)_2]^{2+}$, on the basis of our previous study on the synthesis of Ag-supported silica nanotubes [27].

2. Experimental

2.1. Materials

Calcium carbonate nanoparticles with a mean size of 50 nm in diameter were adopted in the experiments. All the other chemicals used in the experiments were obtained from commercial sources as analytical reagents and used without further purification.

2.2. Preparation of HSNSs

HSNSs were synthesized according to our previously reported paper [26]. In this synthesis, sodium silicate ($Na_2SiO_3 \cdot 9H_2O$) solution was added dropwisely within 2 h into nanosized calcium carbonate suspension (containing ca. 8 wt% $CaCO_3$), which was kept at 353 K and adjusted at pH = 9–10 by simultaneously adding dilute HCl solution to form a core-shell structure with a weight ratio of $SO_2/CaCO_3$ = 10%. After it was further stirred for 2 h at the above conditions, the mixture was filtered and rinsed with distilled water and ethanol, dried at 363 K overnight and calcinated at 873 K for 5 h. The composite was then dissolved into HCl dilute solution (10 wt%) for 12 h to remove the $CaCO_3$ template completely. The resulting gel was then filtered, rinsed again and dried in a vacuum oven to obtain HSNSs.

2.3. Fabrication of Ag-SiO_2 composite hollow nanospheres

To prepare Ag-SO_2 composite hollow nanoparticles, 0.5 g of the as-synthesized HSNSs were immersed in 30 ml of aqueous solution of $[Ag(NH_3)_2]^+$ (prepared by dropwise addition of 25% NH_3 (aq) to 0.2 M $AgNO_3$ solution leading to the formation of a clear colourless solution and then adjusting the pH of the solution to 9.0 or 7.5 with dilute HNO_3) in a brown bottle for 18 h. Subsequently, the samples were filtered and washed thoroughly with deionized

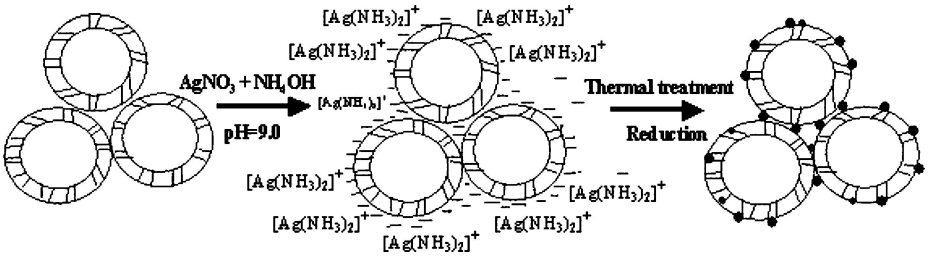

Figure 1 The schematic illustration of the formation process of Ag-supported HSNSs.

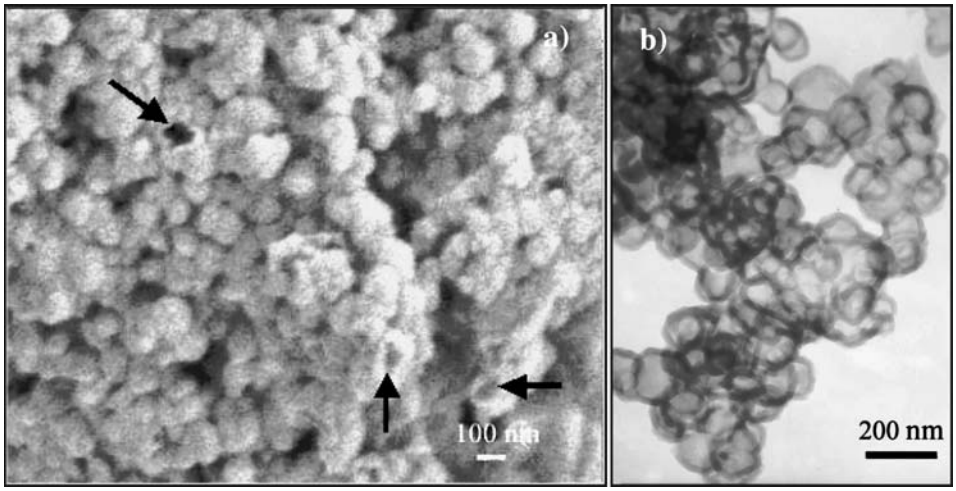

Figure 2 SEM (a) and TEM (b) images of HSNSs.

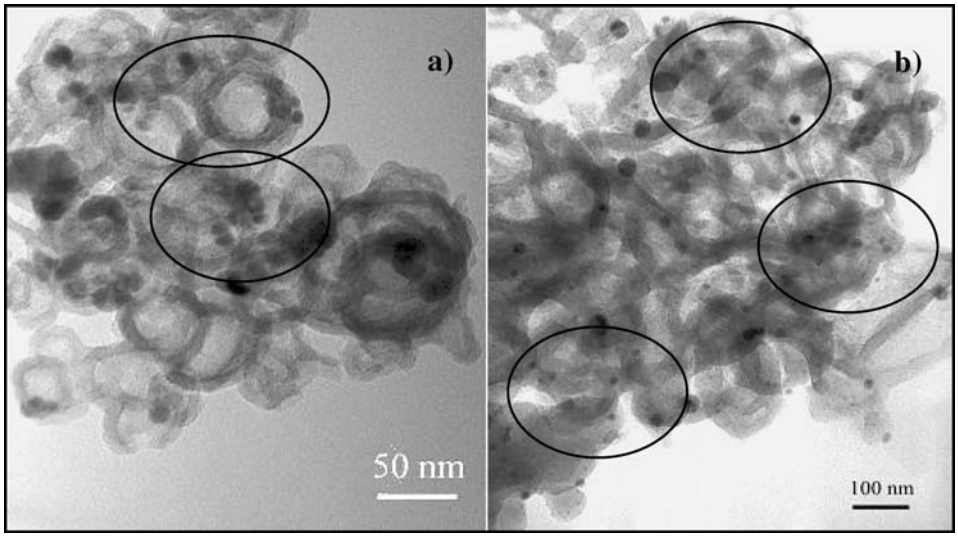

Figure 3 TEM images of Ag-supported HSNSs.

water to remove the solution remaining on the surface. Finally, they were dried under a vacuum condition at a low temperature for 4 h, followed by heating in air to 873 K at 2 K min^{-1} and held for 3 h to generate Ag-supported HSHSs.

2.4. Characterization

The hollow structures of HSNSs were observed by transmission electron microscope (TEM) (HITACHI, H-800), and field emission scanning electron microscope (FE-SEM) (JEOL, JSM-6301F). Direct observation of Ag-supported HSNSs was performed by FE-TEM (JEOL JEM-2010F). The component analysis of the samples was carried out on an Energy Dispersive Spectroscopy (EDS) (LINK, ISIS-300). The Ag loaded amount was examined with a polarized atomic absorption spectrophotometer (AAS) (HITACHI, Z-8000) by dissolving small amount of Ag-supported silica into ammonia water. The Ag-supported sample was studied by X-ray photoelectron spectroscopy (XPS) (Perkin-Elmer, PHI-5300) using MgK_α source at 1253.6 eV. The X-ray powder supply was operated at 250 W (12.5 KV × 20 mA). The pressure in the analysis chamber during scans was kept below 10^{-7} Pa. X-ray diffraction (XRD) measurement was conducted on a diffractometer (Rigaku, D/Max 2500VB2+/PC) with Cu K_α radiation of wavelength 0.154056 nm at a scan speed of 10 ° min^{-1}. The optical absorption spectra were measured by a UV spectrometry (Shimadzu, UV2501-PC).

3. Results and discussion

Fig. 1 shows the schematic illustration of the formation process of Ag-SiO_2 composite hollow nanospheres. It has been demonstrated that silica tends to carry negative charges in a basic solution due to its isoelectric point (IEP) at ∼2 and its zeta potential profile [28]. $[Ag(NH_3)_2]NO_3$

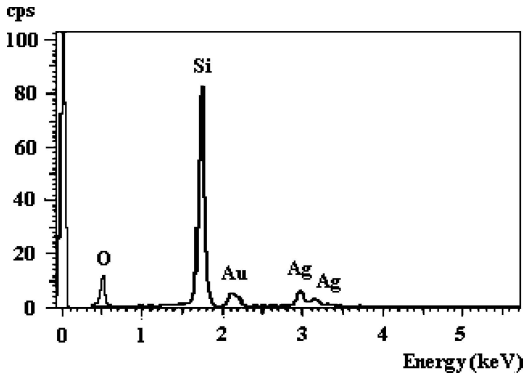

Figure 4 EDS spectrum of Ag-supported HSNSs.

solution would be obtained because of the adjustment of the reaction equilibrium between $AgNO_3$ and NH_4OH with HNO_3. Therefore, the $[Ag(NH_3)_2]^+$ ions were absorbed on the surface of hollow silica by the electrostatic attraction. In addition, the surface of hollow silica spheres with large amount of hydroxyl groups can interact with the NH_3 ligands of the $[Ag(NH_3)_2]^+$ complexes via hydrogen bonds. Upon the heat treatment, $[Ag(NH_3)_2]^+$ would be decomposed and metallic Ag nanoparticles would be reduced and supported on the hollow silica.

The SEM image shown in Fig. 2a reveals that the product consists of well-defined hollow nanospheres with uniform size distribution. Broken hollow spheres can also be observed. To further confirm the hollow nature of the spheres, TEM observations were conducted as well. As shown in Fig. 2b, the light regions in the central parts represent the empty core and the dark edges correspond to the wall of HSNSs [29]. The spherical nanoparticles are at the range of 90–110 nm in diameter and about 15 nm in the wall thickness.

The $[Ag(NH_3)_2]^+$ impregnated samples were colorless after soaking, and exhibited a yellow color after thermal treatment at 873 K. Typical TEM images of Ag-supported

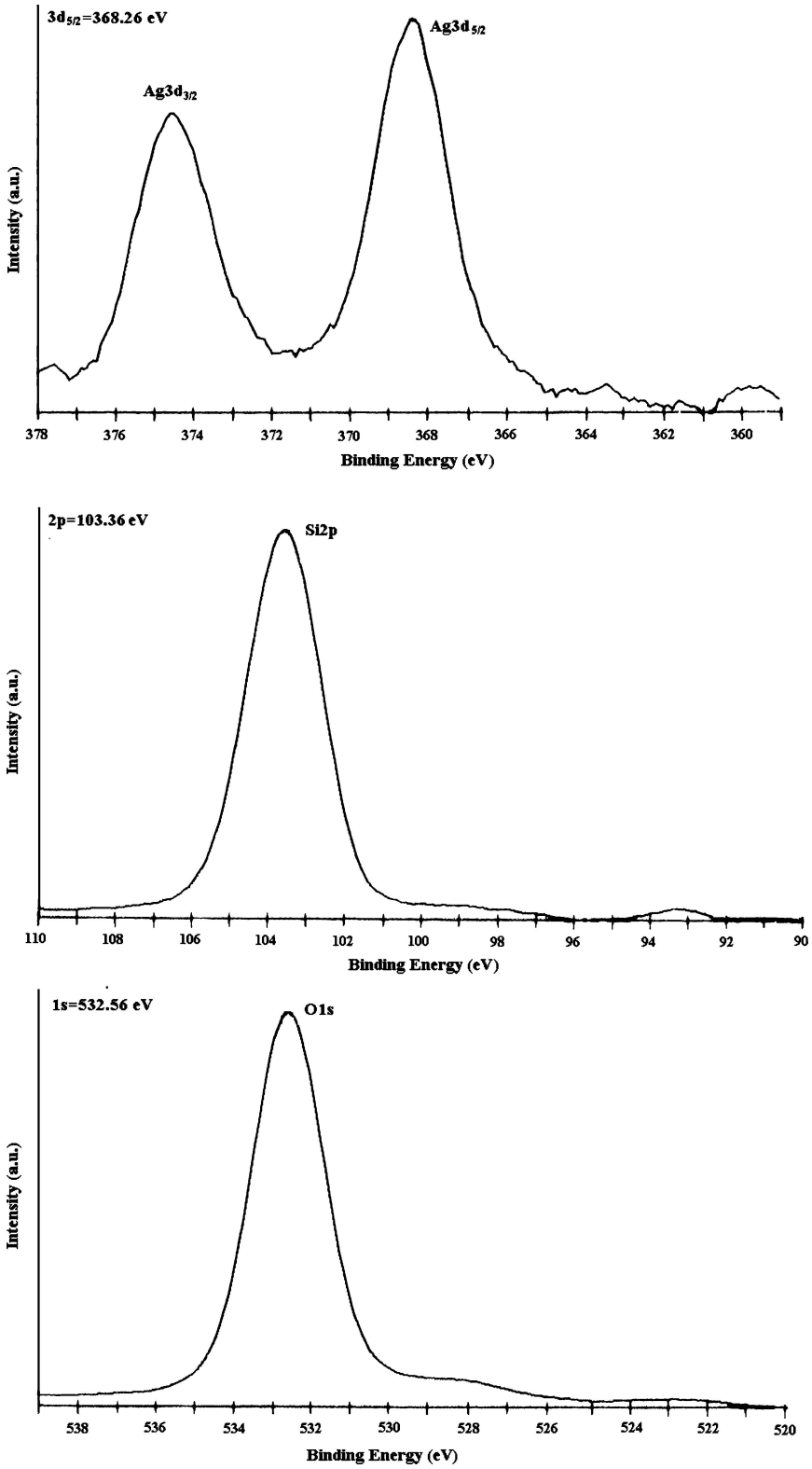

Figure 5 High resolution XPS spectra of Ag-supported HSNSs. (a) Ag, (b) Si, (c) O.

HSNSs are given in Fig. 3a and b. The tiny dark round dots represent Ag nanoparticles with various sizes. From the two TEM images, it can be seen that the Ag nanoparticles have been successfully immobilized on the shells or between the spaces of HSNSs, and they are uniformly dispersed and distributed, with an average particle size of 6–10 nm. Fig. 4 displays the EDS spectrum of Ag-supported HSNSs. It can be seen that in addition to the sputtered Au layer to enhance conductivity, the sample contains only Si, O and Ag, which implies the complete

TABLE I The effect of different $[Ag(NH_3)_2]NO_3$ concentrations and pH values on Ag loadings by AAS

$C_{[Ag(NH_3)_2]^+}$ (M)	pH	Soaking time	C_{Ag^+} (by AAS) (μg/ml)	W_{Ag}
0.02	9.0	18 h	1.10	5.70%
0.08	7.5		1.41	8.50%
0.08	9.0		1.92	9.96%
0.15	9.0		2.15	10.83%

removal of the interior $CaCO_3$ templates and successful immobilization of Ag nanoparticles on HSNSs.

The product purity and elemental composition were determined by XPS. Fig. 5 shows the XPS spectra for Ag-SiO_2 hollow composite. The binding energies obtained in the XPS analysis are standardized for specimen charging using C1s as the reference at 284.6 eV. No peaks of other elements except C, O, Si and Ag are observed on the survey spectrum. High resolution spectra shown in Fig. 5a–c were taken on $Ag3d_{5/2}$, Si2p, and O1s regions. The binding energies are 368.26 eV for $Ag3d_{5/2}$, 103.36 eV for Si2p and 532.56 eV for O1s, respectively. These are assigned to the elements in silica and Ag metal.

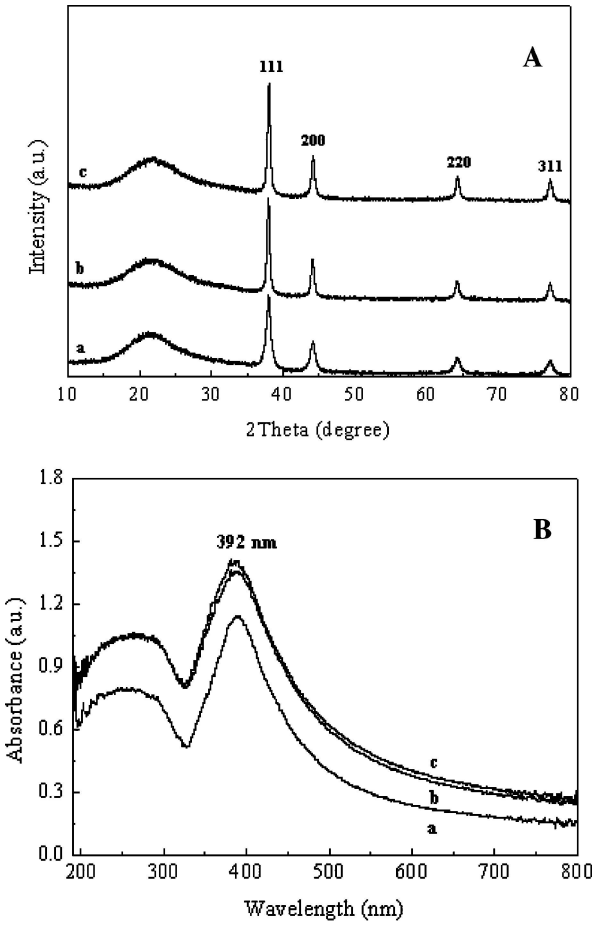

Figure 6 XRD and corresponding UV-Vis patterns of Ag-supported HSNSs after immersing in $[Ag(NH_3)_2]NO_3$ solution with different concentrations at pH = 9.0 for 18 h. (a) 0.02 M, (b) 0.08 M, (c) 0.15 M.

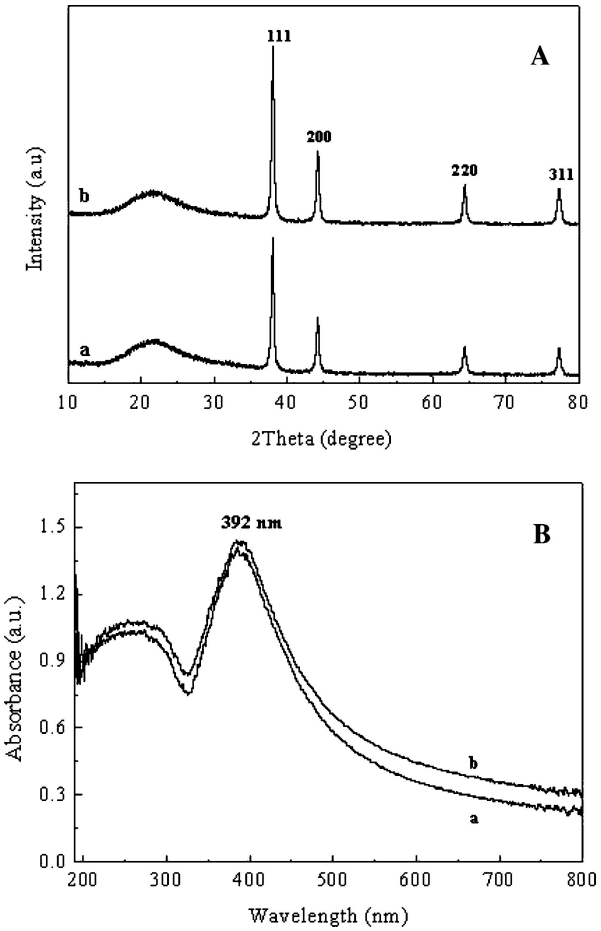

Figure 7 XRD and corresponding UV-Vis patterns of Ag-supported HSNSs after immersing in $[Ag(NH_3)_2]NO_3$ solution (0.08 M) at different pH values for 18 h. (a) 7.5, (b) 9.0.

To further study the influence of loading conditions (concentrations and pH of $[Ag(NH_3)_2]NO_3$ solution) and supports on the immobilization of Ag nanoparticles, AAS, XRD and UV have been utilized to characterize the samples as well.

The loaded amounts of Ag could be calculated with data from AAS by dissolving a little amount of Ag-supported silica into aqueous ammonia. At high basic conditions, small amount of silica will be completely dissolved into the aqueous ammonia after a certain period of time; therefore the loaded Ag nanoprticles will be dispersed into the solution. Hence the loaded amount of Ag can be expressed in weight ratio as:

$$W_{Ag} = \frac{C_{Ag^+} \times V}{M - C_{Ag^+} \times V} \quad (1)$$

where W_{Ag} is the weight of Ag loaded in unit weight of the host material, C_{Ag^+} (measured by AAS) and V (usually 250 ml) are the concentration of Ag^+ ions and the volume of the obtained solution, and M (about 5 mg) is the weight of the weighed Ag-supported HSNSs. Table I shows Ag loadings under different $[Ag(NH_3)_2]NO_3$ concentrations and pH values calculated by the above formula.

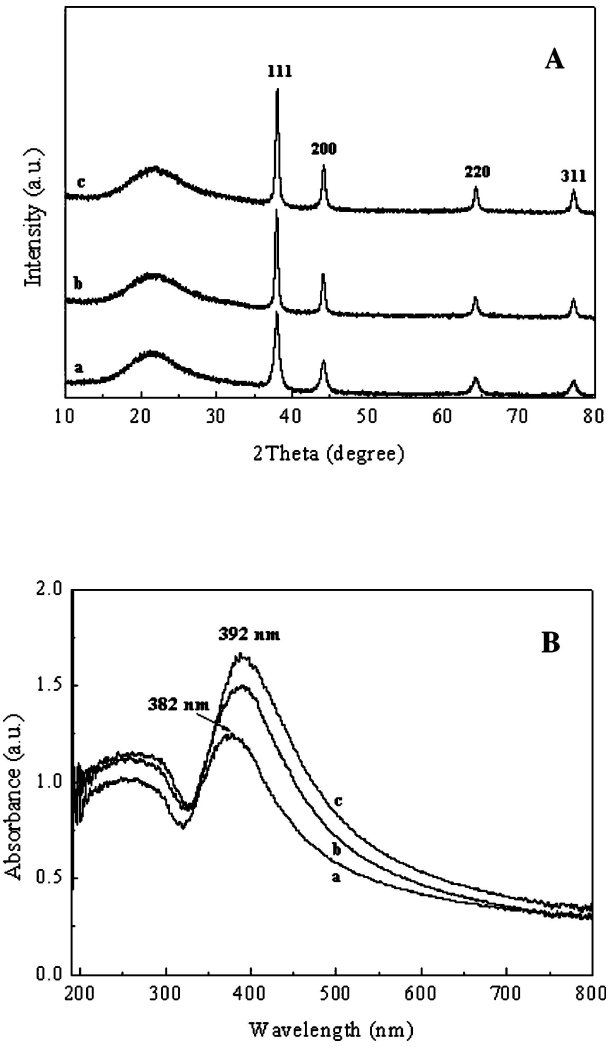

Figure 8 XRD and corresponding UV-Vis patterns of Ag-SiO_2 composite hollow nanospheres prepared from HSNSs with different BET values after immersing in $[Ag(NH_3)_2]NO_3$ solution (0.08 M) at pH = 9.0 for 18 h. (a) 574.6 m^2/g, (b) 734.1 m^2/g, (c) 830.4 m^2/g.

The HSNSs were soaked in $[Ag(NH_3)_2]^+$ solutions with concentrations of 0.02 M, 0.08 M, 0.15 M, respectively, at pH 9.0. The curves for different concentrations of precursor solutions in Fig. 6A show four peaks at 2θ values of 38.1°, 44.3°, 64.5°, 77.5° corresponding to (111), (200), (220), and (311) planes of silver, respectively. There is a broad diffraction peak at around 23°, which corresponds to the amorphous silica matrix. By increasing soaking concentration, the diffraction peaks of silver crystals were more intense. It means that the Ag loading on HSNSs was enhanced. However, when concentration reaches a certain value, Ag loading amount only increases a little, which can be demonstrated by the almost same silver diffraction peak in curve b and c. Therefore, the proper concentration of 0.08 M was employed in the following study to decrease the usage of noble silver. UV-Vis absorption spectra of these composite nanoparticles shown in Fig. 8B were recorded to investigate their optical properties. As can be seen from curve a, b and c, the composite samples have a strong absorption peak at ca. 392 nm corresponding to the surface plasmon resonance (SPR) of Ag nanoparticles (usually peaking in the 380–420 nm range) [30]. By comparison, the intensity of the absorption peak increases in the order c > b > a, and the intensity in curve c is slightly more intense than that in curve b. The result is in good agreement with the data from XRD and AAS.

Fig. 7 reveals XRD and corresponding UV-Vis patterns of Ag-supported HSNSs after immersing in $[Ag(NH_3)_2]NO_3$ solution (0.08 M) at pH = 7.5 and 9.0, respectively. From curve a and b in Fig. 7A, it can be seen that the sample at pH = 9.0 has sharper crystalline silver peaks than that at pH = 7.5. The UV-Vis analysis further confirms the result that more loading of silver can be obtained in the solution with higher pH value, which is in well agreement with the result in Table I. However, too large pH value (pH > 9.0) should be avoided to reduce the undesirable solubility of hollow silica.

Fig. 8 shows XRD and the corresponding UV-Vis patterns of Ag-SiO_2 composite hollow nanospheres prepared from HSNSs with different BET values (Sample a: 574.6 m^2/g; b: 734.1 m^2/g; c: 830.4 m^2/g). From the data of XRD and UV, we can conclude that the Ag amounts loaded on HSNSs would be enhanced with the increment of the BET surface area of HSNSs according to the reinforced intensity of corresponding peaks, due to the larger immobilization area of HSNSs with higher BET.

4. Conclusions

In summary, hollow silica nanospheres prepared by templating nanosized calcium carbonate particles have successfully been employed as a support for immobilization of Ag nanoparticles with $[Ag(NH_3)_2]NO_3$ as silver precursor via heat treatment. The straightforward process yields composite samples containing Ag nanoparticles, with the average size of 6–10 nm in diameter, mainly located on the shells or between the spaces of the HSNSs. The study on the influence of the loading conditions and the hosts on the immobilization of silver indicated that highly efficient loading of silver on HSNSs can be achieved by using hollow silica with large BET as host and 0.08M of $[Ag(NH_3)_2]NO_3$ solution at pH = 9.0 as Ag precursor.

Acknowledgments

The authors gratefully acknowledge the financial support provided by National "863" Program of China (No. 2003AA302620), and National "973" program of China (No. 2003CB615807), the Program for New Century Excellent Talents in University, National Natural Science Foundation of China (Nos. 20325621 and 20236020), Beijing Municipal Commission of Education (JD100100403) and CNPC Innovation Fundation.

References

1. E. MATHLOWITZ, J. S. JACOB, Y. S. JONG, G. P. CARINO, D. E. CHICKERING, P. CHATURVEDL, C. A. SANTOS, K. VIJAYARAGHAVAN, S. MONTGOMERY, M. BASSETT and C. MORRELL, *Nature* **386** (1997) 410.
2. H. HUANG and E. E. REMSEN, *J. Am. Chem. Soc.* **121** (1999) 3805.
3. P. D. YANG, D. Y. ZHAO, B. F. CHMELKA and G. D. STUCKY, *Chem. Mater.* **10** (1998) 1033.
4. H. RINGSDORF, B. SCHLARB and J. VENZMER, *Angew. Chem. Int. Ed. Engl.* **27** (1998) 113.
5. F. CARUSO, R. A. CARUSO and H. MÖHWALD, *Science* **282** (1998) 1111.
6. B. MDISCHER, Y. Y. WON, D. S. EGE, J. C. M. LEE, F. S. BATES, D. E. DISCHER and D. A. HAMMER, *ibid.* **284** (1999) 1143.
7. M. S. WENDLAND and S. C. ZIMMERMAN, *J. Am. Chem. Soc.* **121** (1999) 1389.
8. F. CARUSO, X. Y. SHI, R. A. CARUSO and A. SUSHA, *Adv. Mater.* **13** (2001) 740.
9. B. BOURLINOS, M. A. KARAKASSIDES and D. PETRIDIS, *Chem. Comm.* **16** (2001) 1518.
10. Z. X. WEI and M. X. WAN, *Adv. Mater.* **18** (2002) 1314.
11. D. B. ZHANG, L. M. QI, J. M. MA and H. M. CHENG, *ibid.* **20** (2002) 1499.
12. C. E. FOWLER, D. D. KHUSHALANI and S. MANN, *Chem. Comm.* **19** (2001) 2028.
13. H. T. SCHMIDT and A. E. OSTAFIN, *Adv. Mater.* **14** (2002) 532.
14. D. WALSH, B. LEBEAU and S. MANN, *ibid.* **11** (1999) 324.
15. S. W. KIM, M. KIM, W. Y. LEE and T. HYEON, *J. Am. Chem. Soc.* **124** (2002) 7642.
16. Y. G. SUN, B. MAYERS and Y. N. XIA, *Adv. Mater.* **15** (2003) 641.
17. J. X. HUANG, Y. XIE, B. LI, Y. LIU, Y. T. QIAN and S. Y. ZHANG, *ibid.* **11** (2000) 808.
18. A. B. R. MAYER, W. GREBRIER and R. WANNEMACHER, *J. Phys. Chem. B* **104** (2000) 7278.
19. A. DOLEV, G. E. SHTER and G. S. GRADER, *J. Catal.* **214** (2003) 146.
20. K. C. PARK and S. K. IHM, *Appl. Catal. A-Gen* **203** (2000) 201.
21. D. BABONNEAU, T. CABIOCH, A. NAUDON, J. C. GIRARD and M. F. DENANOT, *Surf. Sci.* **409** (1998) 358.
22. V. HORNEBECQ, M. ANTONIETTI, T. CARDINAL and M. T. DELAPIERRE, *Chem. Mater.* **15** (2003) 1993.
23. M. FERRARI, L. M. GRATTON, A. MADDALENA, M. MONTAGNA and C. TOSELLO, *J. Non-Cryst. Solids* **191** (1995) 101.
24. M. KAWASHITA, S. TSUNEYAMA, F. MIYAJI, T. KOKUBO, H. KOZUKA and K. YAMAMOTO, *Biomaterials* **21** (2000) 393.
25. J. F. CHEN, Y. H. WANG, F. GUO, X. M. WANG and C. ZHENG, *Ind. Eng. Chem. Res.* **39** (2000) 948.
26. J. F. CHEN, J. X. WANG, R. J. LIU, L. SHAO and L. X. WEN, *Inorg. Chem. Comm.* **7** (2004) 447.
27. J. X. WANG, L. X. WEN, Z. H. WANG, M. WANG, L. SHAO and J. F. CHEN, *Scripta Mater.* **51** (2004) 1035.
28. J. P. BRUNELLE, *Pure Appl. Chem.* **50** (1978) 1211.
29. P. V. BRAUN and S. I. STUPP, *Mater. Res. Bull.* **34** (1999) 463.
30. H. ITOIGAWA, T. KAMIYAMA and Y. J. NAKAMURA, *Non-Cryst. Solids* **220** (1997) 210.

Received 18 November 2004
and accepted 12 May 2005